

Tunable band gap in twisted bilayer graphene

Xiu-Cai Jiang,^{1,*} Yi-Yuan Zhao,^{1,*} and Yu-Zhong Zhang^{1,†}

¹*Shanghai Key Laboratory of Special Artificial Microstructure Materials and Technology,
School of Physics Science and Engineering, Tongji University, Shanghai 200092, P.R. China*

(Dated: March 22, 2024)

At large commensurate angles, twisted bilayer graphene which holds even parity under sublattice exchange exhibits a tiny gap. Here, we point out a way to tune this tiny gap into a large gap. We start from comprehensive understanding of the physical origin of gap opening by density functional theory calculations. We reveal that the effective inter-layer hopping, intra-layer CDW, or inter-layer charge imbalance favors a gap. Then, on the basis of tight-binding calculations, we suggest that a periodic transverse inhomogeneous pressure, which can tune inter-layer hoppings in specific regions of the moiré supercell, may open a gap of over 100 meV, which is further confirmed by first-principles calculations. Our results provide a theoretical guidance for experiments to open a large gap in twisted bilayer graphene.

I. INTRODUCTION

Electronic properties of twisted bilayer graphene (tBLG)¹ are strongly affected by moiré pattern and inter-layer coupling². As a result, many exotic phenomena such as Mott insulator^{3,4}, superconductivity⁵⁻⁷, and higher-order topological insulator^{8,9} have been discovered in tBLG with different stacking configurations. Of particular interest, at large commensurate angles, tBLG, which holds even parity under sublattice exchange (SE), has not only graphene-like low-energy spectra^{10,11} but also an intrinsic gap at half filling^{11,12}, making it a promising candidate for high-mobility field effect transistors. However, the gap is too small to switch off electrical conduction at room temperature, which impedes such applications¹³.

Therefore, in order to overcome this problem, much effort has been made to investigate conditions for gap opening at half filling and properties of gapped states. It was proposed for the first time that the ground state of the tBLG with twisted angle $\theta = 38.21^\circ$ is insulating with an intrinsic gap of less than 10 meV at half filling over a decade ago¹¹. Using a long-wavelength theory, Mele pointed out that all SE-even structures are gapped, which are ascribed to pseudo spin-orbit coupling resulting from hoppings between layers^{14,15}. From the tight-binding analyses, it was shown that gap only exists in SE-even tBLG with a twisted angle $\theta > \theta_c \approx 1.89^\circ$ ¹⁶. Thus, the gap can be tuned by twisting different angles between two layers. Besides, in-plane strains can tune the gap as well, where a direct-indirect gap transition occurs under mixed in-plane strains¹⁷. Moreover, recently, SE-even structures with large twisted angles were proposed to be higher-order topological insulators hosting corner states which emerge as long as the underlying symmetries are intact⁸. These findings further trigger the interest to study the gapped state in SE-even tBLG.

However, till now, despite extensive investigations, an effective way to open a large gap in SE-even tBLG has not yet been proposed. In fact, if only twisting is employed between layers, the gap is so small that one needs to control the twisted angle accurately in a clean sam-

ple to observe it at low temperature¹⁸. Fortunately, the twisted angle can be controlled with a remarkable precision of 0.1° in experiments¹⁹⁻²¹. Besides, the techniques to compress the inter-layer distance down to 80%²², to exert an in-plane tensile strain up to 6% without inelastic relaxation²³, and to apply a transverse electric field²⁴ have been mastered. Applying these techniques to tBLG can lead to many novel phenomena, such as pressure dependence of flat bands²⁵⁻²⁷, magnetism induced by pressure at large twisted angle²⁷, direct-indirect gap transition induced by mixed in-plane strains¹⁷, and tunable gap induced by a transverse electric field²⁴. Furthermore, tBLG has intra-layer on-site potential differences²⁸, which are neglected in long-wavelength theory¹⁴ and tight-binding approximation¹⁶. On-site potential differences in the layer often induce an in-plane uneven charge distribution resulting in an intra-layer charge density wave (CDW), which may affect the gap. Hence, clarifying the effect of CDW on gap opening and finding a way to open a large gap in tBLG with above available techniques are topical subjects.

In this paper, we point out a way to tune the tiny gap of tBLG with twisted angle $\theta = 38.21^\circ$ into a large gap. First, to show the tunable properties of gap, using first-principles calculations, we study the effects of external tuning parameters like a transverse homogeneous pressure, an in-plane biaxial tensile strain, or a transverse electric field on gap opening. We find that gap increases monotonously with increasing these tuning parameters. Second, to understand the reasons why gap increases with these parameters, we calculate effective inter-layer hopping and order parameters of intra- and inter-layer charge disproportionation. We reveal that enhancement of gap amplitude with applying pressures or strains is attributed to the increase of both intra-layer CDW and effective inter-layer hopping, where the latter always plays a dominant role on gap opening, while external electric field can induce an inter-layer charge imbalance, resulting in enlargement of the gap. Third, using tight-binding model, we demonstrate how to open a larger gap by tuning inter-layer hoppings, and on-site potentials which can modify intra-layer CDW, in spe-

cific regions of the moiré supercell, respectively. Finally, based on the guidance of tight-binding calculations, we suggest that a periodic transverse inhomogeneous pressure can open a gap of over 100 meV, which is further confirmed by first-principle calculations.

Our paper is organized as follows. Sec. II describe the details of the structure, the model, and the method we used. Sec. III present our main results, including gaps as functions of different external tuning parameters, density of state (DOS) and band structures, contour maps of difference of charge density, effective inter-layer hopping and order parameters of CDW states, analyses of tight-binding calculations and variations of different physical quantities as functions of effective periodic transverse inhomogeneous pressure. Sec. IV includes a discussion of our results and Sec. V concludes with a summary.

II. MODEL AND METHOD

The structure of tBLG with twisted angle $\theta = 38.21^\circ$, which can be realized in experiment²⁹, is shown in Fig. 1(a). According to the atomic environment, we identify three distinct regions in the moiré supercell, namely, A, H, and M region as shown in Fig. 5(a), corresponding to the region where atoms of two layers (green) sits on top of each other, the region where hexagon centers of two layers overlap (pink), and the region of the rests (blue), respectively.

To calculate the properties of tBLG under a transverse homogeneous pressure, an in-plane biaxial tensile strain, a transverse electric field, or a periodic transverse inhomogeneous pressure, density functional theory (DFT) calculations are employed, based on the projector augmented wave method³⁰ as implemented in the Vienna Ab initio Simulation Package (VASP)^{31,32}. We choose the generalized gradient approximation (GGA) of Perdew-Burke-Ernzerhhor³³ to the exchange-correlation potentials with van der Waals correction called vdW-DF2-B86r^{34,35}, which is considered to be the functional with the best overall performance in multi-layer graphene³⁶. A plane-wave energy cutoff of 450 eV is employed. A Γ -centered K-point grid of $45 \times 45 \times 1$ is used in the Brillouin-zone integral. The vacuum distance is set to be 20 Å to eliminate the coupling between periodic images of the layers in the direction perpendicular to the atomic planes.

To demonstrate how to open a large gap by tuning inter-layer hoppings and on-site potentials in distinct regions of the moiré supercell, a simple model is introduced as

$$H = H_D + \delta H_t + \delta H_\Delta. \quad (1)$$

where

$$H_D = \sum_{i\sigma} \Delta_{i\sigma} C_{i\sigma}^\dagger C_{i\sigma} - \sum_{i\sigma} \sum_{j\sigma'}' t_{ijs\sigma'} C_{i\sigma}^\dagger C_{js'\sigma} \quad (2)$$

is the Hamiltonian derived from DFT calculations with tight-binding parameters obtained through transforma-

tion from Bloch space to maximally localized Wannier function basis by using WANNIER90 code^{37,38}. Totally, 28 bands close to the Fermi energy are taken into account for each spin, which are mainly contributed from p_z orbitals of 28 carbon atoms in the moiré supercell. δH_t and δH_Δ are perturbed Hamiltonians that can be viewed as modelling of external perturbations like applying pressures, strains, and electric fields which result in inter-layer hoppings or on-site potentials deviating from their DFT values. Here, δH_t contains five terms while δH_Δ includes three terms,

$$\begin{aligned} \delta H_t &= \delta H_{t_A} + \delta H_{t_M}^1 + \delta H_{t_M}^2 + \delta H_{t_H}^1 + \delta H_{t_H}^2 \\ \delta H_\Delta &= \delta H_{\Delta_A} + \delta H_{\Delta_M} + \delta H_{\Delta_H}, \end{aligned} \quad (3)$$

where

$$\begin{aligned} \delta H_{t_A} &= \delta t_A \sum_{i\sigma} \sum_{\langle s, s' \rangle \in A} C_{i\sigma}^\dagger C_{is'\sigma} \\ \delta H_{t_M}^1 &= \delta t_M^1 \sum_{i\sigma} \sum_{\langle s, s' \rangle \in M} C_{i\sigma}^\dagger C_{is'\sigma} \\ \delta H_{t_M}^2 &= \delta t_M^2 \sum_{i\sigma} \sum_{\langle\langle s, s' \rangle\rangle \in M} C_{i\sigma}^\dagger C_{is'\sigma} \\ \delta H_{t_H}^1 &= \delta t_H^1 \sum_{i\sigma} \sum_{\langle s, s' \rangle \in H} C_{i\sigma}^\dagger C_{is'\sigma} \\ \delta H_{t_H}^2 &= \delta t_H^2 \sum_{i\sigma} \sum_{\langle\langle s, s' \rangle\rangle \in H} C_{i\sigma}^\dagger C_{is'\sigma} \\ \delta H_{\Delta_A} &= \delta \Delta_A \sum_{i\sigma} \sum_{s \in A} C_{i\sigma}^\dagger C_{i\sigma} \\ \delta H_{\Delta_M} &= \delta \Delta_M \sum_{i\sigma} \sum_{s \in M} C_{i\sigma}^\dagger C_{i\sigma} \\ \delta H_{\Delta_H} &= \delta \Delta_H \sum_{i\sigma} \sum_{s \in H} C_{i\sigma}^\dagger C_{i\sigma}. \end{aligned} \quad (4)$$

Here, i (j), s (s'), and σ denote cell, sublattice, and spin index, respectively. $\langle s, s' \rangle$ ($\langle\langle s, s' \rangle\rangle$) means the summation over inter-layer nearest (next-nearest)-neighbor sites. δt_A , δt_M^1 , δt_M^2 , δt_H^1 , and δt_H^2 are the deviations of inter-layer hopping integrals in corresponding regions (see Fig. 5(a)) from their DFT values due to external perturbations, while $\delta \Delta_A$, $\delta \Delta_M$, and $\delta \Delta_H$ stand for the deviations of on-site potentials in corresponding regions from their DFT values. Thus, using this model, we can study the effect of external perturbations, which affect inter-layer hoppings or on-site potentials in distinct regions of the moiré supercell, on gap opening.

III. RESULTS

Now, we start with the tunable properties of the gap in SE-even tBLG with twisted angle of $\theta = 38.21^\circ$. Fig. 1(b) shows gap as a function of inter-layer distance d , where intra-layer C-C bond length $a = 1.42$ Å is adopted. As can be seen, the system is always gapped despite the differences in the inter-layer distance. The gap increases monotonously with decrease of d , which can be effec-

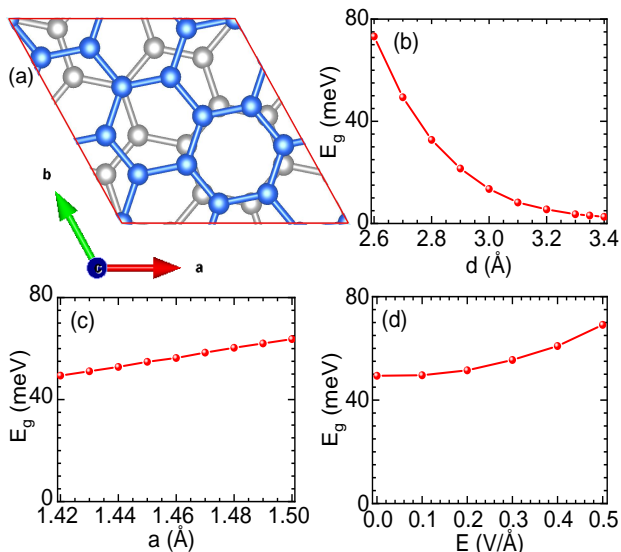


FIG. 1. (a) Structure of SE-even tBLG with twisted angle $\theta = 38.213^\circ$. (b) Gap as a function of d , where $a=1.42$ Å is used. (c) Gap as a function of a , where $d=2.7$ Å is adopted. (d) Gap as a function of gated field E , where $a=1.42$ Å and $d=2.7$ Å are used.

tively viewed as applying transverse homogeneous pressure. We estimate the magnitude of the pressure to be 30 GPa when $d = 2.7$ Å. Therefore, gap of the system is tunable by a transverse homogeneous pressure. It is worth noting that gap of the equilibrium geometry of tBLG is of 3.1 meV, which is comparable with the results obtained from other first-principles calculations¹¹ and long-wavelength theory¹⁴ but is not coincident with the result of tight-binding approximation where unreasonable large gap was obtained¹⁶. Band gap opening is further confirmed by DOS and band structures as presented in Fig. 2(a) ($d = 2.7$ Å only) and Fig. 2(b) respectively.

To show the effect of an in-plane biaxial tensile strain on gap opening of the system, we have calculated gap as a function of intra-layer C-C bond length a as shown in Fig. 1(c), where $d = 2.7$ Å is used. We find gap increasing monotonously with the increase of a , indicating that gap increases monotonously with an applied in-plane biaxial tensile strain. The same conclusion is obtained by other first-principles calculations when the inter-layer distance is fixed at the equilibrium distance¹⁷. Band gap opening is further confirmed by band structures as illustrated in Fig. 2(c). Therefore, gap is tunable by an in-plane biaxial tensile strain.

A transverse electric field can induce symmetry breaking between top and bottom layers, which may tune gap of the system. Fig. 1(d) shows the gap as a function of a transverse electric field, where $a = 1.42$ Å and $d = 2.7$ Å are used. We find that gap of the system increases monotonously with an applied transverse electric field, which is consistent with the results observed in experiment²⁴ and that obtained by tight-binding model³⁹, but

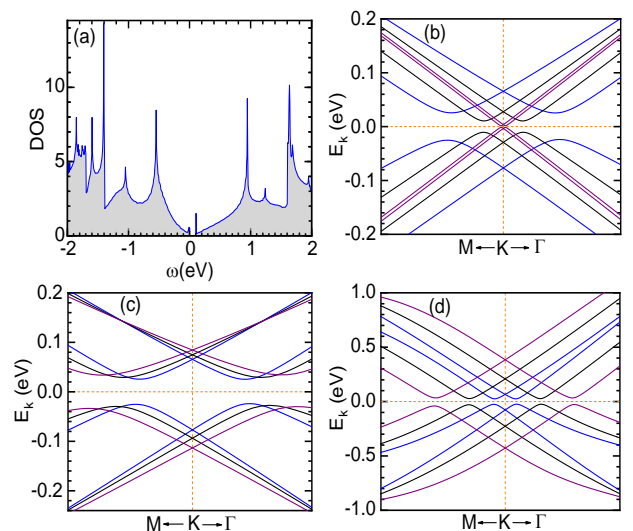


FIG. 2. (a) Total density of states for $a=1.42$ Å, $d=2.7$ Å. (b) Band structures for different inter-layer distances with 2.7 Å (blue), 2.9 Å (black) and 3.35 Å (purple), where $a=1.42$ Å is used. (c) Band structures for different bond lengths with 1.42 Å (blue), 1.46 Å (black) and 1.50 Å (purple), where $d=2.7$ Å is adopted. (d) Band structures for different gated fields with 0.0 V/Å (blue), 0.2 V/Å (black) and 0.4 V/Å (purple), where $a=1.42$ Å and $d=2.7$ Å are used.

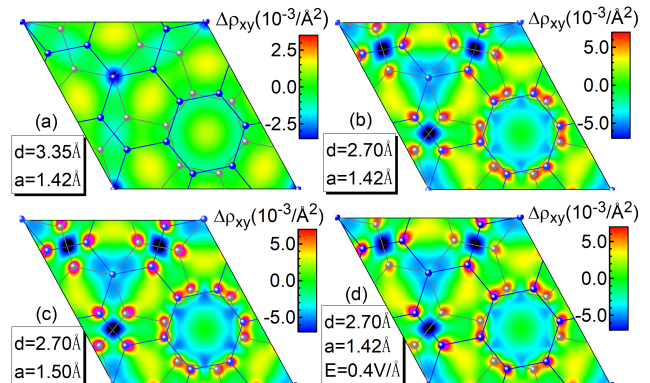


FIG. 3. Contour maps of charge density difference between tBLG and superposition of two individual graphene layers for different structures with $d=3.35$ Å, $a=1.42$ Å in (a), $d=2.70$ Å, $a=1.42$ Å in (b), $d=2.70$ Å, $a=1.50$ Å in (c) and $d=2.70$ Å, $a=1.42$ Å, $E=0.4$ V/Å in (d), respectively. Note that the scale of the color bar in (a) is half of that in (b)-(d).

is contrary to the conclusion obtained by continuum approximation where gapless state remains in the presence of gated electric field⁴⁰. Band structures under different transverse electric field are presented in Fig. 2(d). Thus, an electric field can tune the gap as well.

It is worth noting that an intrinsic intra-layer CDW exists in the system, which has not yet been mentioned. Besides, an inter-layer charge imbalance occurs when applying a transverse electric field. To illustrate this, we show

the contour maps of charge density difference between tBLG and superposition of two individual graphene layers where charges are equally distributed at all sites for different structures in Fig. 3. Interestingly, there is an uneven charge distribution in tBLG even with the structure of equilibrium geometry as shown in Fig. 3(a), indicating existence of an intrinsic intra-layer CDW. As we can see from Figs. 3(b) and 3(c), the uneven charge distribution enhances when applying a transverse homogeneous pressure and an in-plane biaxial tensile strain, respectively. Furthermore, when applying a transverse electric field, Fig. 3(d) exhibits an additional imbalance of charge distribution between top (blue) and bottom (gray) layer compared with the case without electric field (Fig. 3(b)), indicating the formation of an inter-layer charge imbalance. In fact, an intra-layer CDW or an inter-layer charge imbalance plays a crucial role in gap opening. Therefore, clarifying the effect of inter-layer hoppings, intra-layer CDW and inter-layer charge imbalance on gap opening is the key to obtain a larger gap in tBLG.

Next, we proceed to demonstrate that, the gap size increasing with reduced inter-layer distance or strengthened in-plane biaxial tensile strain is attributed to the increase of both intra-layer CDW and effective inter-layer hopping, where the latter always dominates gap opening, while gap is enlarged by the gated electric field due to the formation of an inter-layer charge imbalance.

A transverse homogeneous pressure can push the top and bottom layers closer together, which enhances both inter-layer hybridizations and Coulomb interactions, leading to the increase of effective inter-layer hopping and intra-layer CDW. In order to quantify the strength of inter-layer hoppings and intra-layer CDW, we have calculated effective inter-layer hopping t_{eff} , defined as the band splitting at the K point of Brillouin zone in the absence of intra-layer CDW, and order parameter of the intra-layer CDW $\Delta n_t = \sum_s |n_s - 1.0|$ as functions of d in Fig. 4(a), where \sum_s sums over the sublattices in the supercell. Obviously, t_{eff} and Δn_t increase monotonously with reduced inter-layer distance. As a result, both the gap induced by effective inter-layer hopping alone E_g^{NCDW} , where the effect of intra-layer CDW is removed artificially, and the gap caused by intra-layer CDW $E_g - E_g^{NCDW}$ (gray shadow) increase with the transverse homogeneous pressure as shown in Fig. 4(d). Thus, the real gap of the system E_g increase monotonously with the transverse homogeneous pressure. Moreover, one can see that the effective inter-layer hopping dominates the gap opening.

An in-plane biaxial tensile strain stretches the in-plane C-C bond a , resulting in the decrease of intra-layer hybridizations, indicating that p_z electrons around the C atoms are more localized in the intra-layer direction while more extended in the inter-layer direction. As a result, the effective inter-layer hopping increases due to the increased overlap between wave functions of two layers, and the intra-layer CDW is enhanced since electrons are more localized in the intra-layer direction, which are con-

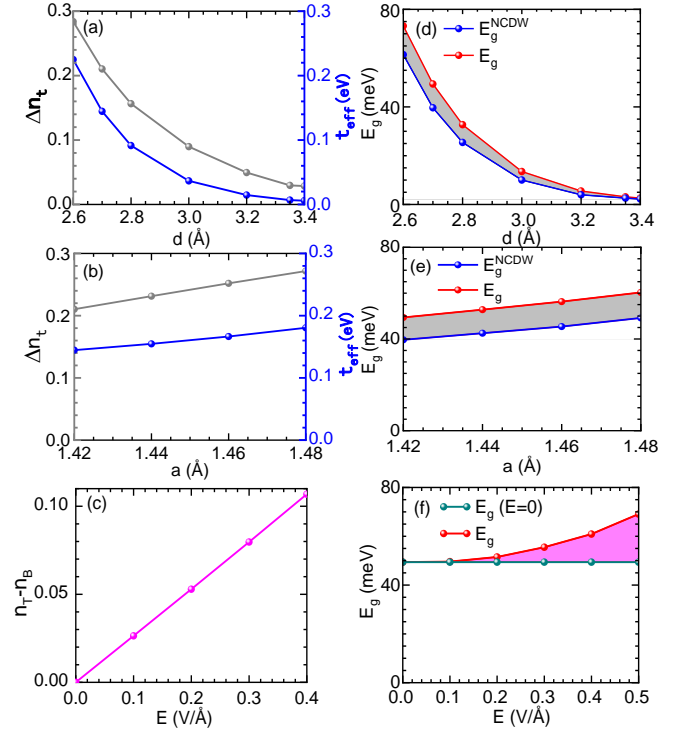


FIG. 4. (a) and (b) show the effective inter-layer hopping t_{eff} and order parameter of the intra-layer CDW Δn_t as functions of d and a respectively. (c) Order parameter of the inter-layer charge imbalance $n_T - n_B$ as a function of E . (d) and (e) present E_g^{NCDW} and E_g as functions of d and a respectively. E_g^{NCDW} is the gap induced by inter-layer hoppings alone, where the effect of intra-layer CDW is removed artificially, while E_g is the real gap of the system. NCDW is the abbreviation of no charge density wave. (f) E_g as a function of E , where $E_g(E=0)$ is the gap without electric field. $a=1.42 \text{ \AA}$ is used in (a) and (d), $d=2.70 \text{ \AA}$ is used in (b) and (e), $d=2.70 \text{ \AA}$ and $a=1.42 \text{ \AA}$ are used in (c) and (f). The calculation method of t_{eff} for different structures are shown in Fig. 7 of Appendix A and Fig. 8 of Appendix B.

firmed by our calculations on effective inter-layer hopping t_{eff} and order parameter of the intra-layer CDW Δn_t as functions of a in Fig. 4(b). Therefore, through a similar analysis as we did in the case of applying transverse homogeneous pressure, we reveal that the E_g increasing monotonously with the in-plane biaxial tensile strain, as shown in Fig. 4(e), can be ascribed to the increase of both intra-layer CDW and effective inter-layer hopping, where the latter always dominates the gap opening.

An (downward) electric field perpendicular to tBLG layers generates an electric potential difference between the top and bottom layers, which leads to electronic charge transfer from the bottom to top layer. We have calculated order parameter of inter-layer charge imbalance $n_T - n_B = \sum_s^T n_s - \sum_{s'}^B n_{s'}$ as a function of E in Fig. 4(c), where \sum_s^T and $\sum_{s'}^B$ sum over the sublattices of top and bottom layer in the supercell, respectively. We find that $n_T - n_B$ increases monotonously with the

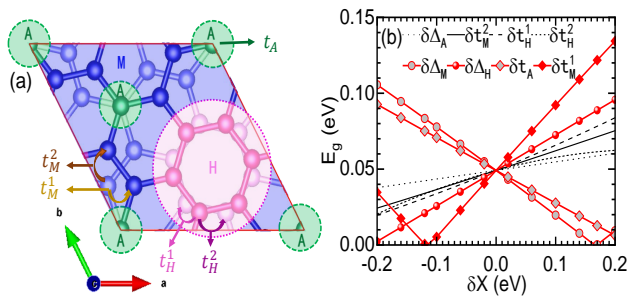


FIG. 5. (a) Three distinct regions, namely, A (green) region, M (blue) region, and H (pink) region in the moiré supercell. (b) Gaps as functions of the deviations of inter-layer hoppings and on-site potentials δX , including δt_A , δt_M^1 , δt_M^2 , δt_H^1 , δt_H^2 , $\delta\Delta_A$, $\delta\Delta_M$, and $\delta\Delta_H$ as described in Eq. (4), which are used to simulate the effect of external perturbations. Gap at $\delta X = 0$ corresponds to the gap of $d = 2.7$ Å and $a = 1.42$ Å.

electric field. As a result, the gap is further opened as shown in Fig. 4(f), where $E_g - E_g(E = 0)$ (pink shadow) is the gap induced by the inter-layer charge imbalance. Therefore, we reveal that gap increasing with the electric field is due to the formation of an inter-layer charge imbalance.

In brief, gap of the system is tunable by inter-layer distance, in-plane biaxial strain and gated electric field since those can increase the effective inter-layer hopping, intra-layer CDW, or inter-layer charge imbalance. However, simply applying these external perturbations cannot open a large gap in the system. Fortunately, the effective inter-layer hopping and intra-layer CDW depend on various inter-layer hybridizations and intra-layer on-site potentials in different regions of the supercell (see Fig. 5(a)), respectively, which provides additional degrees of freedom to tune the gap. Therefore, in the following, we will demonstrate how to open a larger gap by tuning inter-layer hybridizations and on-site potentials in specific regions of the moiré supercell.

According to the lattice structure of tBLG we studied, totally five inter-layer hopping terms between neighboring sites within same region as defined in Fig. 5(a) and three different on-site potential terms for three different regions are believed to dominate the inter-layer hoppings and intra-layer CDW. Thus, we introduce perturbations to these terms as shown in Sec. II. In Fig. 5(b), we present gap amplitude as functions of these perturbations at $d = 2.7$ Å and $a = 1.42$ Å. It is found that the gap increases dramatically as δt_M^1 and $\delta\Delta_H$ increase or δt_A and $\delta\Delta_M$ decrease. Therefore, to open a larger gap in this system experimentally, one needs to enhance t_M^1 and Δ_H , meanwhile weaken t_A and Δ_H . Since above DFT calculations demonstrate that effective inter-layer hopping dominates the gap opening, we would like to propose that applying a periodic transverse inhomogeneous pressure which affect t_M^1 and t_A in opposite direction may be a promising way to obtain a large gap.

Finally, we will verify above proposal by first-principles

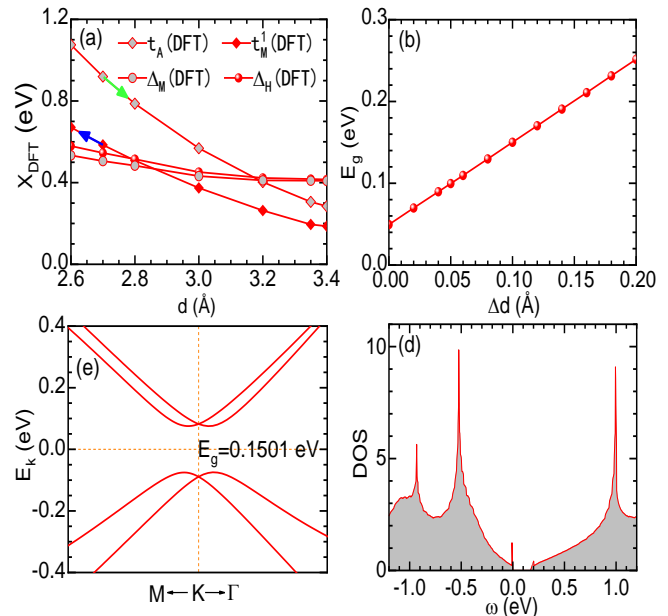


FIG. 6. (a) The DFT values of t_A , t_M^1 , Δ_M , and Δ_H as functions of d . (b) Gap as a function of the height difference between A and M regions within the same layer Δd , where inter-layer distances of $d_A = 2.7$ Å + Δd , $d_M = 2.7$ Å - Δd , and $d_H = 2.7$ Å are used. (c) and (d) illustrate the band structure and density of state of the case $\Delta d = 0.1$ Å respectively.

calculations. In Fig. 6(a), it is shown that both t_M^1 and t_A increase with decrease of d , indicating that, by enlarging the inter-layer distance of A region d_A and compressing that of M region d_M as shown by the colored arrow in Fig. 6(a), one may fulfill the requirement of increasing t_M^1 and decreasing t_A simultaneously. To demonstrate this, we perform DFT calculations on tBLG with region-dependent inter-layer distances of $d_A = 2.7$ Å + Δd , $d_M = 2.7$ Å - Δd , and $d_H = 2.7$ Å, which can be effectively viewed as applying a periodic transverse homogeneous pressures. Fig. 6(b) presents the gap as a function of Δd . It is found that the gap is larger than 100 meV when $\Delta d \geq 0.05$ Å. Interestingly, the band structure still satisfies the nearly linear low-energy spectra as illustrated in Fig. 6(c). The gap is of 150.1 meV when $\Delta d = 0.1$ Å, which is further confirmed by the DOS in Fig. 6(d). Therefore, a periodic transverse inhomogeneous pressure is an efficient way to open a larger gap in this system.

IV. DISCUSSION

Here, combining first-principle calculations with tight-binding calculations, we point out a way to open a large gap in tBLG with twisted angle $\theta = 38.21^\circ$. All of our calculations are performed without the consideration of spin polarization since the DOS of this system near the Fermi surface is too small to stabilize a magnetic ground

state. When the twisted angle is not so large, tBLG under a large transverse pressure will favor a correlated ferromagnetic ground state due to the occurrence of the flat bands²⁷. However, flat bands do not exist in our case.

Our paper mainly focuses on the tBLG with twisted angle $\theta = 38.21^\circ$. To our knowledge, the properties of tBLG are strongly dependent on the twisted angle between two layers based on model analyses. The low-energy spectra are quite different for SE-even tBLG and SE-odd tBLG, where the former is gapped while the latter is gapless due to symmetry⁴¹. While an in-plane shift of one layer with respect to the other may turn SE-even tBLG into SE-odd tBLG resulting in gap close, SE-even tBLG is stable and can be realized in experiment²⁹. We have also done calculations on tBLG with twisted angle $\theta = 46.83^\circ$. It is found that the gap also increase quickly when applying a transverse homogeneous pressure as illustrated in Fig. 9 of Appendix C. Thus, it is interesting to study the properties of tBLGs with other twisted angles based on first-principles calculations. However, it is beyond the scope of the present paper.

Interestingly, we have proposed here for the first time that there is an intrinsic intra-layer CDW in SE-even tBLG with large twisted angle, which has not yet been mentioned. In fact, the intra-layer on-site potential differences affect mainly the low-energy spectra of tBLG as shown in Fig. 7 of Appendix A and Fig. 8 of Appendix B. However, the intra-layer on-site potential differences are neglected in long-wavelength theory¹⁴ and tight-binding approximation¹⁶. As a result, flat bands with broken electron-hole symmetry, which are different from that obtained by tight-binding approximation, are observed by DFT calculations²⁷. Therefore, we strongly suggest that it is necessary to include the effect of intra-layer CDW in long-wavelength theory and tight-binding approximation to study the low-energy properties of tBLG.

We have shown that applying a periodic transverse inhomogeneous pressure leads to region-dependent inter-layer distances and consequently enhance the gap. Perhaps this is not difficult to achieve in experiments. It has been observed that deposition of C₆₀ on tBLG can increase the gap of tBLG from 35 to 80 meV due to the increased concentration of inter-layer C-C bonding⁴². Moreover, we would like to propose that deposition of polar molecule may lead to region-dependent on-site potentials which may favor gapped state. It is worth noting that not only does the tBLG we studied can open a large band gap under a periodic transverse inhomogeneous pressure, but it still maintains nearly linear dispersion of low-energy spectra, indicating the high electron mobility still remains.

It is worth mentioning that the band gaps of semiconductors are systematically underestimated by DFT calculations⁴³. Thus, the actual band gap given by experiment may be larger than the calculated one in tBLG.

V. CONCLUSION

At large commensurate angles, tBLG which holds even parity under sublattice exchange exhibits a tiny gap. Here, we point out a way to tune this tiny gap into a larger gap. First, from first-principles calculations, we find that the gap size increases with increasing transverse homogeneous pressures, in-plane biaxial tensile strains, or transverse electric fields. We reveal that enhancement of the gap by pressures or strains is attributed to the increases of both intra-layer CDW and effective inter-layer hopping, while it is due to the formation of an inter-layer charge imbalance under applied electric fields. Then, using a tight-binding model, we demonstrate how to open a larger gap by tuning inter-layer hoppings and on-site potentials in specific regions of the moiré supercell. Finally, based on the guidance of tight-binding calculations, we propose that a periodic transverse inhomogeneous pressure can open a gap of over 100 meV, which is further confirmed by first-principles calculations. Our results provide a theoretical guidance for experiments to open a large gap in tBLG, and may pave a way for carbon-based electronics.

ACKNOWLEDGEMENT

This work is supported by National Natural Science Foundation of China (Nos.11774258, 12004283) and Shanghai Science and technology program (No.21JC405700).

Appendix A: The t_{eff} for structures with different d

Fig. 7 shows the band structures of tBLG with and without the effect of intra-layer CDW for structures with different d , where the effective inter-layer hopping t_{eff} for different d are given. As can be seen, t_{eff} increases monotonously with the decrease of d .

Appendix B: The t_{eff} for structures with different a

Fig. 8 shows the band structures of tBLG with and without the effect of intra-layer CDW for structures with different a , where the effective inter-layer hopping t_{eff} for different a are also given. It is to easy find that, t_{eff} increases monotonously with the increase of a .

Appendix C: Tunable gap in tBLG with twisted angle $\theta = 46.83^\circ$

Fig. 9 shows the band structures of tBLG with twisted angle $\theta = 46.83^\circ$. When without a transverse homogeneous pressure ($d = 3.35 \text{ \AA}$), as can be seen in Fig. 9(a), the gap of the system $E_g = 0.6 \text{ meV}$. The gap increase quickly under a transverse homogeneous pressure

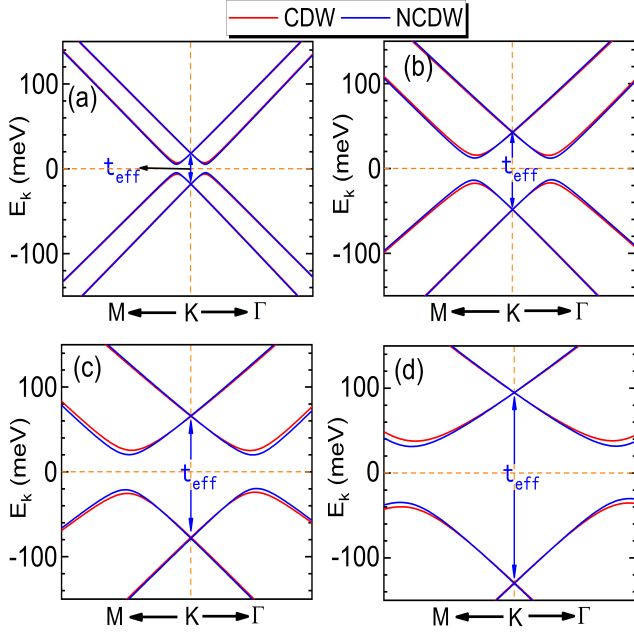


FIG. 7. At twisted angle $\theta = 38.21^\circ$, band structures of tBLG with and without the effect of intra-layer CDW for different d , $d = 3.35 \text{ \AA}$, $d = 2.8 \text{ \AA}$, $d = 2.7 \text{ \AA}$, and $d = 2.6 \text{ \AA}$ are used in (a), (b), (c), and (d) respectively. $a = 1.42 \text{ \AA}$ is adopted in all cases.

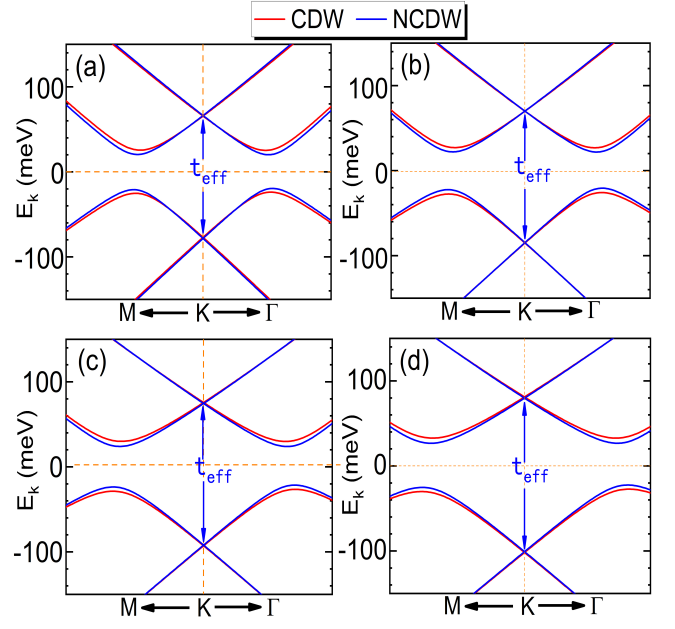


FIG. 8. At twisted angle $\theta = 38.21^\circ$, band structures of tBLG with and without the effect of intra-layer CDW for different a , $a = 1.42 \text{ \AA}$, $a = 1.44 \text{ \AA}$, $a = 1.46 \text{ \AA}$, and $a = 1.48 \text{ \AA}$ are used in (a), (b), (c), and (d) respectively. $d = 2.7 \text{ \AA}$ is adopted in all cases

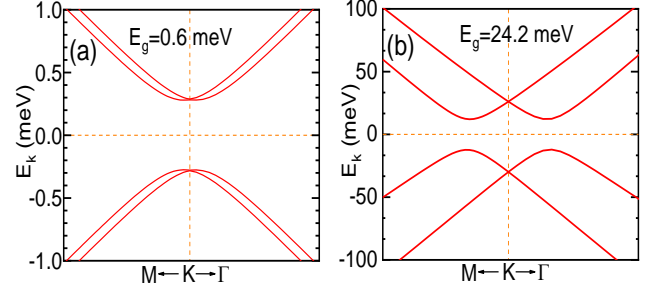


FIG. 9. Band structure of tBLG with twisted angle $\theta = 46.83^\circ$, $d = 3.35 \text{ \AA}$ and $d = 2.7 \text{ \AA}$ are used in (a) and (b) respectively, where $a = 1.42 \text{ \AA}$ is used.

($d = 2.7 \text{ \AA}$), where the system is gapped with a gap of 24.2 meV in Fig. 9(b).

* These authors contribute equally to the paper.

† Corresponding author. Email: yzzhang@tongji.edu.cn

¹ Alexandr Vladimirovich Rozhkov, AO Sboychakov, AL Rakhmanov, and Franco Nori, “Electronic properties of graphene-based bilayer systems,” *Physics Reports* **648**, 1–104 (2016).

² Taisuke Ohta, Jeremy T. Robinson, Peter J. Feibelman, Aaron Bostwick, Eli Rotenberg, and Thomas E. Beechem, “Evidence for interlayer coupling and moiré periodic potentials in twisted bilayer graphene,” *Phys. Rev. Lett.* **109**, 186807 (2012).

³ Yuan Cao, Valla Fatemi, Ahmet Demir, Shiang Fang, Spencer L Tomarken, Jason Y Luo, Javier D Sanchez-Yamagishi, Kenji Watanabe, Takashi Taniguchi, Efthimios Kaxiras, *et al.*, “Correlated insulator behaviour at half-filling in magic-angle graphene superlattices,” *Nature* **556**, 80–84 (2018).

⁴ Hoi Chun Po, Liujun Zou, Ashvin Vishwanath, and T Senthil, “Origin of mott insulating behavior and superconductivity in twisted bilayer graphene,” *Physical Review X* **8**, 031089 (2018).

- ⁵ Yuan Cao, Valla Fatemi, Shiang Fang, Kenji Watanabe, Takashi Taniguchi, Efthimios Kaxiras, and Pablo Jarillo-Herrero, “Unconventional superconductivity in magic-angle graphene superlattices,” *Nature* **556**, 43–50 (2018).
- ⁶ Xiaobo Lu, Petr Stepanov, Wei Yang, Ming Xie, Mohammed Ali Aamir, Ipsita Das, Carles Urgell, Kenji Watanabe, Takashi Taniguchi, Guangyu Zhang, *et al.*, “Superconductors, orbital magnets and correlated states in magic-angle bilayer graphene,” *Nature* **574**, 653–657 (2019).
- ⁷ Leon Balents, Cory R Dean, Dmitri K Efetov, and Andrea F Young, “Superconductivity and strong correlations in moiré flat bands,” *Nature Physics* **16**, 725–733 (2020).
- ⁸ Moon Jip Park, Youngkuk Kim, Gil Young Cho, and SungBin Lee, “Higher-order topological insulator in twisted bilayer graphene,” *Physical review letters* **123**, 216803 (2019).
- ⁹ M Kindermann, “Topological crystalline insulator phase in graphene multilayers,” *Physical review letters* **114**, 226802 (2015).
- ¹⁰ Mike Sprinkle, David Siegel, Yike Hu, J Hicks, Antonio Tejada, Amina Taleb-Ibrahimi, Patrick Le Fèvre, François Bertran, S Vizzini, H Enriquez, *et al.*, “First direct observation of a nearly ideal graphene band structure,” *Physical Review Letters* **103**, 226803 (2009).
- ¹¹ S Shallcross, Sangeeta Sharma, and Oleg A Pankratov, “Quantum interference at the twist boundary in graphene,” *Physical review letters* **101**, 056803 (2008).
- ¹² S. Shallcross, S. Sharma, E. Kandelaki, and O. A. Pankratov, “Electronic structure of turbostratic graphene,” *Phys. Rev. B* **81**, 165105 (2010).
- ¹³ Jeroen B Oostinga, Hubert B Heersche, Xinglan Liu, Alberto F Morpurgo, and Lieven MK Vandersypen, “Gate-induced insulating state in bilayer graphene devices,” *Nature materials* **7**, 151–157 (2008).
- ¹⁴ Eugene J Mele, “Commensuration and interlayer coherence in twisted bilayer graphene,” *Physical Review B* **81**, 161405 (2010).
- ¹⁵ EJ Mele, “Interlayer coupling in rotationally faulted multilayer graphenes,” *Journal of Physics D: Applied Physics* **45**, 154004 (2012).
- ¹⁶ A. O. Sboychakov, A. L. Rakhmanov, A. V. Rozhkov, and Franco Nori, “Electronic spectrum of twisted bilayer graphene,” *Phys. Rev. B* **92**, 075402 (2015).
- ¹⁷ Zahra Khatibi, Afshin Namiranian, and Fariborz Parhizgar, “Strain impacts on commensurate bilayer graphene superlattices: Distorted trigonal warping, emergence of bandgap and direct-indirect bandgap transition,” *Diamond and Related Materials* **92**, 228–234 (2019).
- ¹⁸ AV Rozhkov, AO Sboychakov, AL Rakhmanov, and Franco Nori, “Single-electron gap in the spectrum of twisted bilayer graphene,” *Physical Review B* **95**, 045119 (2017).
- ¹⁹ Y Cao, JY Luo, V Fatemi, S Fang, JD Sanchez-Yamagishi, K Watanabe, T Taniguchi, E Kaxiras, and Pablo Jarillo-Herrero, “Superlattice-induced insulating states and valley-protected orbits in twisted bilayer graphene,” *Physical review letters* **117**, 116804 (2016).
- ²⁰ Kyoungwan Kim, Matthew Yankowitz, Babak Fallahazad, Sangwoo Kang, Hema CP Movva, Shengqiang Huang, Stefano Larentis, Chris M Corbet, Takashi Taniguchi, Kenji Watanabe, *et al.*, “van der waals heterostructures with high accuracy rotational alignment,” *Nano letters* **16**, 1989–1995 (2016).
- ²¹ Kyoungwan Kim, Ashley DaSilva, Shengqiang Huang, Babak Fallahazad, Stefano Larentis, Takashi Taniguchi, Kenji Watanabe, Brian J LeRoy, Allan H MacDonald, and Emanuel Tutuc, “Tunable moiré bands and strong correlations in small-twist-angle bilayer graphene,” *Proceedings of the National Academy of Sciences* **114**, 3364–3369 (2017).
- ²² You Xiang Zhao and Ian L Spain, “X-ray diffraction data for graphite to 20 gpa,” *Physical Review B* **40**, 993 (1989).
- ²³ Ke Cao, Shizhe Feng, Ying Han, Libo Gao, Thuc Hue Ly, Zhiping Xu, and Yang Lu, “Elastic straining of free-standing monolayer graphene,” *Nature communications* **11**, 1–7 (2020).
- ²⁴ Jing-Bo Liu, Ping-Jian Li, Yuan-Fu Chen, Ze-Gao Wang, Fei Qi, Jia-Rui He, Bin-Jie Zheng, Jin-Hao Zhou, Wan-Li Zhang, Lin Gu, *et al.*, “Observation of tunable electrical bandgap in large-area twisted bilayer graphene synthesized by chemical vapor deposition,” *Scientific reports* **5**, 1–9 (2015).
- ²⁵ Stephen Carr, Shiang Fang, Pablo Jarillo-Herrero, and Efthimios Kaxiras, “Pressure dependence of the magic twist angle in graphene superlattices,” *Physical Review B* **98**, 085144 (2018).
- ²⁶ Liangbing Ge, Kun Ni, Xiaojun Wu, Zhengping Fu, Yalin Lu, and Yanwu Zhu, “Emerging flat bands in large-angle twisted bi-layer graphene under pressure,” *Nanoscale* **13**, 9264–9269 (2021).
- ²⁷ Felix Yndurain, “Pressure-induced magnetism in rotated graphene bilayers,” *Physical Review B* **99**, 045423 (2019).
- ²⁸ Nikita V Tepliakov, QuanSheng Wu, and Oleg V Yazyev, “Crystal field effect and electric field screening in multilayer graphene with and without twist,” *Nano Letters* (2021).
- ²⁹ Elad Koren, Itai Leven, Emanuel Lörtcher, Armin Knoll, Oded Hod, and Urs Duerig, “Coherent commensurate electronic states at the interface between misoriented graphene layers,” *Nature nanotechnology* **11**, 752–757 (2016).
- ³⁰ P. E. Blöchl, “Projector augmented-wave method,” *Phys. Rev. B* **50**, 17953–17979 (1994).
- ³¹ G. Kresse and J. Furthmüller, “Efficient iterative schemes for ab initio total-energy calculations using a plane-wave basis set,” *Phys. Rev. B* **54**, 11169–11186 (1996).
- ³² Georg Kresse and Jürgen Furthmüller, “Efficiency of ab-initio total energy calculations for metals and semiconductors using a plane-wave basis set,” *Computational materials science* **6**, 15–50 (1996).
- ³³ John P. Perdew, Kieron Burke, and Matthias Ernzerhof, “Generalized gradient approximation made simple,” *Phys. Rev. Lett.* **77**, 3865–3868 (1996).
- ³⁴ Kyuho Lee, Éamonn D. Murray, Lingzhu Kong, Bengt I. Lundqvist, and David C. Langreth, “Higher-accuracy van der waals density functional,” *Phys. Rev. B* **82**, 081101 (2010).
- ³⁵ Iktaro Hamada, “van der waals density functional made accurate,” *Phys. Rev. B* **89**, 121103 (2014).
- ³⁶ Rafael R Del Grande, Marcos G Menezes, and Rodrigo B Capaz, “Layer breathing and shear modes in multilayer graphene: a dft-vdw study,” *Journal of Physics: Condensed Matter* **31**, 295301 (2019).
- ³⁷ Nicola Marzari, Arash A. Mostofi, Jonathan R. Yates, Ivo Souza, and David Vanderbilt, “Maximally localized wannier functions: Theory and applications,” *Rev. Mod. Phys.* **84**, 1419–1475 (2012).

- ³⁸ Arash A Mostofi, Jonathan R Yates, Young-Su Lee, Ivo Souza, David Vanderbilt, and Nicola Marzari, “wannier90: A tool for obtaining maximally-localised wannier functions,” *Computer physics communications* **178**, 685–699 (2008).
- ³⁹ AO Sboychakov, AV Rozhkov, AL Rakhmanov, and Franco Nori, “Externally controlled magnetism and band gap in twisted bilayer graphene,” *Physical review letters* **120**, 266402 (2018).
- ⁴⁰ JMB Lopes Dos Santos, NMR Peres, and AH Castro Neto, “Graphene bilayer with a twist: Electronic structure,” *Physical review letters* **99**, 256802 (2007).
- ⁴¹ E. J. Mele, “Band symmetries and singularities in twisted multilayer graphene,” *Phys. Rev. B* **84**, 235439 (2011).
- ⁴² Jeongho Park, William C Mitchel, Said Elhamri, Lawrence Grazulis, John Hoelscher, Krishnamurthy Mahalingam, Choongyu Hwang, Sung-Kwan Mo, and Jonghoon Lee, “Observation of the intrinsic bandgap behaviour in as-grown epitaxial twisted graphene,” *Nature communications* **6**, 1–8 (2015).
- ⁴³ Ferdi Aryasetiawan and Olle Gunnarsson, “The GW method,” *Reports on Progress in Physics* **61**, 237 (1998).